Title: Development of ASG-15ME, a Novel Antibody Drug Conjugate Targeting *SLITRK6*, a New Urothelial Cancer Biomarker

Kendall Morrison, Pia M. Challita-Eid, Arthur Raitano, Zili An, Peng Yang, Joseph D. Abad, Wendy Liu, Dawn Ratay Lortie, Josh T. Snyder, Linnette Capo, Alla Verlinsky, Hector Aviña, Fernando Doñate, Ingrid B. J. Joseph, Daniel S. Pereira, Karen Morrison, David R. Stover.

Author Affiliations: all authors are affiliated with Agensys Inc.

Running Title: Therapeutic ADC Targeting *SLITRK6* in Bladder Cancer

Keywords: Bladder Cancer, Antibody Drug Conjugate, SLITRK6, Monomethyl auristatin E, Metastatic bladder cancer

Financial Statement; All authors listed are employees of Agensys and no funding was obtained from other sources

Corresponding Author: Kendall Morrison, Agensys Inc. 1800 Stewart Street, Santa Monica, CA 90405, U.S.A. Phone: 424-280-5191; Fax: 424-280-5046; E-mail: kmorrison@agensys.com

Disclosure of Potential Conflicts of Interest; The authors disclose no potential conflicts of interest

Abstract

SLITRK6 is a member of the SLITRK family of neuronal transmembrane proteins that was discovered as a bladder tumor antigen using suppressive subtractive hybridization. Extensive immunohistochemistry showed SLITRK6 to be expressed in multiple epithelial tumors including bladder, lung and breast cancer as well as in glioblastoma. To explore the possibility of using SLITRK6 as a target for an antibody drug conjugate (ADC) we generated a panel of fully human monoclonal antibodies specific for SLITRK6. ADCs showed potent in vitro and in vivo cytotoxic activity after conjugation to Monomethyl Auristatin E or Monomethyl Auristatin F. The most potent ADC, ASG-15ME, was selected as the development candidate and given the product name AGS15E. ASG-15ME is currently in Phase I Clinical Trials for the treatment of metastatic urothelial cancer. This is the first report that SLITRK6 is a novel antigen in bladder cancer and also the first report of the development of ASG-15ME for the treatment of metastatic bladder cancer.

Introduction

Recent advances in the antibody-drug conjugate (ADC) technology and two recently approved ADCs have brought this drug class to the forefront of drug development in oncology. ADCETRIS® (brentuximab vedotin) was approved in 2011 for the treatment of relapsed Hodgkin lymphoma and systemic anaplastic large cell lymphoma (1,2) and KADCYLA® (ado-trastuzumab emtansine) was approved in 2013 for the treatment of Her2 positive metastatic breast cancer (3,4,5).

Although KADCYLA® and ADCETRIS® may have broader application than the indications for which they have been approved (6, 7), these expansion indications will not include bladder cancer as neither CD30 nor Her-2 have been reported to be expressed in this difficult to treat disease. Bladder cancer is the second most common cancer of the genitourinary tract and the ninth most common cancer in the world with over 430,000 cases diagnosed worldwide in 2012 (8). According to the American Cancer Society there will be over 76,000 new cases of bladder cancer diagnosed and over 15,000 deaths from advanced bladder cancer in the United States in 2014 (9). Approximately 75–85% of patients with bladder cancer present with disease that is confined to the mucosa [stage Ta, carcinoma *in situ* (CIS)] or submucosa (stage T1). Of these, approximately 70% present as stage Ta, 20% as T1 and 10% as CIS (10). These superficial tumors can be completely removed by transurethral resection but there is a high risk of recurrence. Approximately 50-70 % of patients will develop tumor recurrence within 5 years and almost 90% will have a recurrence of their disease by 15 years (11). Patients who develop invasive disease (approximately 25%) have a five-year survival rate of 60% for T2 tumors, 35% for T3 tumors and 10% for T4 tumors. More aggressive, recurrent, bladder cancer requires more severe treatments such as radiotherapy, neoadjuvant chemotherapy or radical cystectomy (12).

Poor prognosis and ineffective therapies for patients with advanced bladder cancer make the discovery of new drugs very important for the treatment of this common disease.

We have developed a novel ADC that is currently in Phase I Clinical Trials for the treatment of advanced urothelial cancer. ASG-15ME (Product name, AGS15E) is composed of a *SLITRK6*-specific human gamma 2 antibody (Igγ2) conjugated to MMAE via a protease-cleavable linker. SLITRK6 was discovered as a bladder tumor antigen using suppressive subtractive hybridization (SSH) on biopsies from bladder cancer patients. The gene has an open reading frame of 841 amino acids and was identified as SLITRK6, a member of the SLITRK family of proteins. The SLITRK family members are type I transmembrane proteins that share conserved leucine-rich repeat domains similar to those in the secreted axonal guidance molecule, SLIT. They also show similarities to Ntrk neurotrophin receptors in their carboxy-termini, sharing a conserved tyrosine residue (13). This family has 6 members and most data provided about their expression has come from embryonic and knockout mouse studies. RNA studies of human brain and fetal tissue show that the SLITRK family members are expressed mainly in the brain, with the exception of SLITRK6 which has been shown, through RNA studies, also to be seen in lung and liver (14). More recent studies have shown SLITRK6 to be involved in development of the inner ear neural circuit in mice (15, 16). SLITRK6 mutations have been shown to cause myopia and deafness in humans and mice (17).

We report here the discovery that SLITRK6 is expressed at high levels in bladder cancer and to a lesser extent in other epithelial tumors (lung, breast and glioblastoma). In addition we discuss the pre-clinical development of ASG-15ME along with the rationale for developing it as a new treatment for advanced bladder cancer.

Materials and Methods

Immunohistochemical Analysis of SLITRK6 Expression in Bladder Cancer and Normal Tissues

Evaluation of SLITRK6 expression in tumor and normal tissues was performed using the mouse monoclonal antibody M15-68(2)22 (murine Igγ2). This antibody was developed at Agensys after immunizing balb/c mice (Charles River) with a peptide specific for a portion of the SLITRK6 extracellular domain (aa274-284). Specificity of the Agensys-developed mouse anti-human SLITRK6 monoclonal antibody M15-68(2)22 was investigated in a series of immunohistochemical (IHC) assays on formalin-fixed, paraffin-embedded (FFPE) tissues and cell pellets (See Supplemental Data; Agensys generated IHC Reagent M15-68(2)22). A non-binding murine antibody was used as a negative control (Sigma). Briefly, slides were de-waxed and antigen retrieval was carried out using Citra (Biogenex) in the E-Z Retriever microwave (Biogenex) for 45 minutes at 95°C. Sections were transferred to the i6000 auto-stainer (Biogenex) and incubated with 3% hydrogen peroxide followed by serum free protein blocking solution (Dako) for 20 minutes to inhibit endogenous peroxidase. M15-68(2)22 or a murine Igγ2 isotype control antibody, at a concentration of 0.5μg/ml, were then applied for 1 hour at room temperature. Detection was with Super Sensitive Polymer-HRP kit (Biogenex) using diaminobenzidine (DAB) as the chromogen. Sections were counterstained with hematoxylin and dehydrated before application of a cover-slip.

The intensity and extent of SLITRK expression by IHC on tissue microarrays (TMAs) was determined microscopically using the histochemical scoring system (H-score). H-score was calculated by summing the products of the staining intensity (0-3) and the percentage of cells

stained at a given intensity (0-100) (18). The results were then assigned into one of 4 groups as follows: High (H-score ≥ 200); Moderate (H-score 100 to 199); Low (H-score 15 to 99); Negative (H-score ≤15).

A total of 509 formalin fixed paraffin embedded (FFPE) biopsies, representing all stages of bladder cancer, were examined in a series of TMAs obtained from US Biomax or Tristar Technology Group.

The normal tissue expression profile of SLITRK6 was examined using TMAs containing 37 different human tissues including those recommended in the FDA normal tissue panel. These were tested with M15-68(2)22 using the same IHC conditions as described above.

Generation of SLITRK6-Specific Human Monoclonal Antibodies (mAbs)

A large panel of SLITRK6 specific human antibodies was generated by immunizing Xenomice™ with either cells expressing SLITRK6 or recombinant SLITRK6 protein. Lymph node cells from immunized mice were fused with Sp2/0-AG14 B-cell hybridoma cells (ATCC) by electro cell fusion using an ECM2100 electro cell manipulator (BTX). SLITRK6 specific hybridomas were identified by screening supernatants by ELISA or by FACS (BD Biosciences) on SLITRK6 positive 3T3 cells or a panel of cell lines with known expression of SLITRK6. AGS-15C, the parental antibody used to create ASG-15ME, was generated after immunizing human Igγ2 producing mice with the murine fibroblast cell line 3T3 (ATCC) engineered to express human SLITRK6.

Cloning of AGS-15C

Total RNA was extracted from AGS-15C producing hybridoma cells using a Trizol® Reagent (Life Technologies) according to the manufacturer's protocol. cDNA was generated using RACE cDNA amplification kit (Clontech) and reverse primer within the constant region of the human light and heavy chains as per the manufacturer's protocol. The amplified variable heavy chain and kappa light chain regions were sequenced and cloned into the pEE12.4 mammalian cell expression vector encoding the full-length human IgG2 and kappa constant domains (Lonza). This plasmid was transfected into CHOK1-SV host cells (Lonza) according to manufacturer's protocol. Transfected cells were selected in absence of glutamine to generate a stable cell line producing AGS-15C.

Generation of the ASG-15ME and other SLITRK6 Specific ADCs

AGS-15C and other SLITRK6 specific antibodies, as well as negative control antibodies, were conjugated with MMAE through a protease-cleavable valine-citrulline (vc) dipeptide linker or with Monomethyl Auristatin F (MMAF) via a non-cleavable maleimidocaproyl-containing (mc) linker, as previously described (19, 20). ASG-15ME is the name used for AGS-15C after conjugation with valine-citrulline MMAE (vcMMAE) and AGS-15MF is the name for maleimidocaproyl MMAF (mcMMAF) conjugated AGS-15C. Other antibodies in the panel have an E or an F as the last letter in their names depending on if they are conjugated with MMAE or MMAF. ADCs tested had a drug-to- antibody ratio (DAR) of approximately 4:1.

Binding Comparison of ASG-15ME and AGS-15C by FACS

FACS analysis to determine maximum binding (B_{max}) and affinity of ASG-15ME (ADC) and AGS-15C (unconjugated mAb) was carried out to ensure that conjugation did not affect binding.

Analysis was carried out on SW-780 cells, a bladder transitional cell carcinoma cell line which endogenously expresses SLITRK6. The SW-780 cell line was obtained from ATCC (catalog # CRL-2169) on Nov. 29, 2011. The cell line was authenticated by short tandem repeat (STR) profiling and tested negative for mycoplasma and mouse pathogens (IMPACT I test). STR authentication profiling was carried out by GE Healthcare, SeqWright Genomic Services using Promega Powerplex 16HS kit on July 24th 2013. For the assay, antibodies were serially diluted and incubated with SW-780 cells (50,000 cells per well) at a final concentration of 40.0 nM to 0.00067 nM and added to the SW-780cells for overnight incubation at 4°C. The incubation was carried out at 4^0C to ensure saturation and this temperature has been shown not to detrimentally affect the performance of the cells. After incubation, phycoerythrin conjugated goat antihuman IgG (Jackson ImmunoResearch Laboratories) was used to detect bound ASG-15ME and AGS-15C. Histograms of each dilution point were generated and the mean fluorescence Intensity (MFI) values were recorded. MFI values were entered into Graphpad Prism software and analyzed using the one site binding (hyperbola) equation of $Y=B_{max}*X/ (K_d+ X)$ to generate saturation curves (K_d was defined as the concentration of each antibody required to reach half-maximal binding).

Confocal Internalization Studies

Confocal microscopy was used to study internalization kinetics of ASG-15ME. In brief, SW-780 cells were seeded onto 4-well polystyrene chamber slides ($4.0x10^4$ cells per well) and grown for 48 hours. Cells were then incubated with 10µg/ml ASG-15ME ADC for 1 hour at 4°C (reduced internalization) or 1 hour at 37°C (rapid internalization). After the incubation period, cells were fixed and permeabilized in Cytofix/Cytoperm™ (BD Biosciences) solution for 20 min at 4°C. Cell surface bound and internalized ASG-15ME was visualized using Alexa Fluor® 488-labeled

goat anti-human IgG (Invitrogen). Lysosomes were visualized by staining with lysosome-associated membrane protein 1, LAMP1 (clone D2D11 XP® Rabbit mAb #9091, Cell Signaling Technology) and a secondary antibody, Alexa Fluor® 488-labeled goat anti-rabbit IgG (Invitrogen). Early endosomes were visualized with endosome marker EEA1 (clone C45B10 rabbit mAb #3288, Cell Signaling Technology). Nuclei were visualized with TOPRO®-3 Iodide (Invitrogen). High-resolution image sections were acquired using a Leica TCS SP5-II Confocal microscope.

In vitro Cytotoxicity Testing of ASG-15ME

ASG-15ME was tested for its ability to kill several SLITRK6 positive cell lines in vitro. The most robust killing was seen in the neuroblastoma cell line CHP-212 and this was used for cytotoxicity assessment of ASG-15ME. CHP-212 cells were obtained from ATCC (catalog # CRL-2273) on May 8, 2012. IGR-OV1 cell line was obtained from NCI on December 21, 2010

Briefly, serially diluted test samples were mixed with the CHP-212 cells in a 96-well plate and incubated for 120 hours in a humidified CO_2 incubator. PrestoBlue® cell viability reagent was used to assess cell viability at the end of the incubation. The viability of CHP-212 cells treated with ASG-15ME was compared to that of target negative cells (IGR-OV1) or cells treated with an isotype control antibody to determine EC_{50} values. The IGR-OV1 cell line was obtained from NCI on December 21, 2010. Authentication STR profiling of CHP-212 cells and IGR-OV1 was carried out on June 21st 2012 and May 26th 2011 respectively.

Immunohistochemical Analysis of SLITRK6 Expression in Xenograft Models

Several patient-derived (PDX) and cell line-derived (CDX) xenograft models were evaluated for SLITRK6 expression using the IHC reagent M15-68(2)22. Staining was carried out on FFPE

sections using the same process as that used to assess SLITRK6 expression in TMAs and normal tissues as described above.

In vivo Activity of SLITRK6-Specific ADCs

CDX models were established by subcutaneous injection of between 2 and 10 million SW780, RT4 (ATCC) or NCI-H322M (NCI) cells in SCID mice. PDX models were established by subcutaneous implantation of xenograft fragments (AG-B7 or AG-B8) in the flanks of SCID mice. Dosing started when tumors reached a size of 200 mm^3 and Study Director Software v2.1 (Studylog Systems Inc.) was used for animal size matching purposes. Female ICR-SCID (Taconic Biosciences) mice, with weight between 20 and 30g, were used in all studies. Expression profiles of cells used for xenograft model establishment are assessed for target expression by RNA analysis and protein analysis when they are received at Agensys. Following this, target expression is monitored by IHC through multiple in vivo passages to ensure that there is no loss of target expression or change in phenotype. In addition, cells used in xenograft model establishment are impact tested (for identification of pathogens) at IDEXX Biosciences.

Dosing was performed by intravenous injection and ADCs tested were conjugated to either vcMMAE or mcMMAF. Non-binding, isotype matched, control ADC or vehicle control were used in each experiment. Caliper measurements of tumors were taken twice per week for the duration of the study. Tumor volume was calculated using the following formula;

$width^2 \times length/2 = volume\ (mm^3)$

All experimental protocols were approved by Agensys' Institutional Animal Use Committee (IACUC). The last day of study was the day on which control animal tumor sizes had exceeded the maximum volume allowed in the study protocol. After this study animals were euthanized.

Statistical Analysis

Xenograft data were analyzed using SAS software (Cary, NC). A statistical analysis of the tumor volume data for the last day immediately before animal sacrifice was performed using the nonparametric Kruskal-Wallis test. Pairwise comparisons were made using the Tukey-Kramer method (2-sided) on the ranks of the data to protect experiment-wise error rate (21).

Results

SLITRK6 is Highly Expressed in Bladder Cancer TMAs

A total of 509 cases of bladder cancer were investigated using TMAs. Overall, SLITRK6 expression was seen in 88% of the bladder cancer specimens of which 67% had strong to moderate expression. When tumors were categorized by histopathological diagnosis, SLITRK6 expression was seen in 90% of transitional cell carcinoma cases, 100% of metastatic bladder cancer cases and 54% of other bladder cancer types (Table 1a). Other types of bladder cancer included squamous cell and adenocarcinoma. Expression in these subtypes was not as strong as that seen in transitional cell carcinoma and metastatic bladder cancer. Of the 16 cases of adenocarcinoma, five had weak staining for SLITRK6 and the rest were negative. Of the 17 squamous cell carcinoma cases, one was classified as strong, two as moderate, nine weak and five negative.

Several of the biopsies in the TMAs had been graded according to the TNM (tissue node metastasis) system. Scoring in the system indicates how deeply the tumor has penetrated the bladder wall (T stage), whether it has reached the nodes (N) and whether it metastasized to other parts of the body (M); these stages are then grouped as 0 through 4 (11). T_0 denotes carcinoma in situ (T_{is}) and is pre-invasive. Invasive bladder cancer is stage T_1 or greater, meaning that the

tumor has invaded the lining of the bladder. If the tumor has invaded the muscle layer of the bladder, it is stage T_2. Stage T_3 cancer has grown through the bladder muscle into the fat layer surrounding the bladder, while stage T_4 cancer has spread to nearby organs.

Within the arrays there were a total of 425 specimens with TNM grades. Of these, 125 specimens had a grade between 0 and 1 and 300 specimens with a TNM grade of 2-4 (Table 1b). The majority of cases, irrespective of stage, had moderate to strong SLITRK6 expression suggesting that there is no correlation between stage and expression of SLITRK6.

In all specimens examined specific immunoreactivity was observed predominantly on cell membranes or on cell membranes and in the cytoplasm of tumor cells (Figure 1a).

In all 125 cases with a TNM score of 0-1, 77% had an H-score > 100 as shown in a representative specimen in Figure 1b and only 6% of cases were negative. Of the 300 cases with a TNM grade of 2-4, 65% had an H-score > 100 (Figure 1c and 1d) and only 10% of cases were negative. Altogether >90% of tumors were positive in grades 0 through 4 and 100% of metastatic bladder cancer cases (n=18) were positive (Figure 1e).

SLITRK6 is Expressed in Few Normal Tissues

Tissue micro-arrays representing 37 normal tissues were examined by IHC. No expression was seen in most tissues tested (Table 2). Specific and strong SLITRK6 expression was seen transitional epithelium of bladder and ureter where staining was strong, membranous and homogenous (Figure 2a). Other normal tissues where we saw staining were adrenal gland, stomach and pancreas where staining was weak and diffuse. Six adrenal gland specimens were examined and all appeared to have some staining for SLITRK6; however, staining was cytoplasmic and weak in most cases. Two specimens did have some areas where staining was

more intense but once again signal was only seen in the cytoplasm (Figure 2b). Six stomach specimens were examined and all had some cytoplasmic staining which was of weak to moderate intensity in glandular epithelium of the basal mucosa (Figure 2c). Staining was seen in 5 of 6 pancreas specimens but staining was cytoplasmic and weak and in a few cases a few acinar cells appeared positive with weak to moderate cytoplasmic staining (Figure 2d). There were also some positive areas in normal lung, colon and breast but these appeared to be nonspecific as the staining was in very few areas while other areas with similar structures e.g. bronchioles and crypts were completely negative. (Figure 2e).

In addition, individual isolated cell staining was seen in interstitial cells in multiple organs including bladder, breast, colon, esophagus, fallopian tube, lung, rectum, salivary gland, skin, small intestine and uterine cervix (Figure 2f). Morphologically these appeared to be mast cells and this was confirmed by double staining for mast cell tryptase.

AGS-15C was Selected from a Panel of Over 70 SLITRK6-Specific mAbs

AGS-15C was chosen from a panel of seven lead mAbs selected from a large panel of over 70 SLITRK6-specific antibodies. It was selected from a panel of gamma 1 and gamma 2 antibodies representing different epitope BIN groups and affinities (Table 3). Epitope bin groups were determined by competition binding studies (data not shown). The majority of mAbs in the original panel (over 70 mAbs) were gamma1 and only a few were gamma 2. We speculated that the selection of AGS-15C as the lead (a human gamma 2 antibody) may be due to better pharmacokinetic properties and thus better exposure. Further experiments would need to be done to prove this.

Conjugation of AGS-15C with MMAE did not Inhibit Binding to SLITRK6

Binding of AGS-15C mAb was compared with three lots of ASG-15ME ADC. AGS-15C antibody shows high affinity binding to SLITRK6 expressed on SW780 cells with a K_d of 0.015 nM (Table 4). No reduction in B_{max} or K_d was observed after conjugation with MMAE and the three ADC lots tested look similar to AGS-15C (Table 4).

ASG-15ME Internalizes After Binding to SLITRK6

Confocal microscopy was used to visualize the internalized ASG-15ME after binding to SW780 cells. At 4^0C, ASG-15ME showed distinct membrane localization (Figure 3a, bright green). After one hour incubation at 37°C, membrane localization of ASG-15ME was dramatically reduced and the ADC appeared as discrete intracellular aggregates throughout the cytosol (Figure 3a). These studies confirmed that ASG-15ME is rapidly internalized after binding to cell surface SLITRK6. Trafficking of ASG-15ME to lysosomes and early endosomes was visualized using a LAMP1 specific antibody and an EEA1 specific antibody respectively (Figure 3b). Lysosomes visualized with LAMP1 appeared as discrete cytosolic vesicles (green). ASG-15ME could be visualized with a similar cytosolic distribution after 30 minutes at 37^oC (red). Punctate intra-cellular ASG-15ME co-localized with LAMP1 can be seen by yellow spots (denoted by arrows) showing that ASG-15ME is trafficked to the lysosomes. ASG-15ME was also shown to co-localization with early endosome marker, EEA1 further confirming the endocytosis and probable hydrolysis of ASG-15ME after internalization.

Figure 3c shows a FACS histogram of ASG-15ME (Lot # 1389-39-A used for internalization studies) binding to SLITRK6 on SW780 cells (purple).

In vitro Cytotoxicity Testing of ASG-15ME

ASG-15ME was tested for its ability to kill several SLITRK6 positive cell lines. The most robust killing was seen with the neuroblastoma cell line CHP-212. SW-780 was also tested but it was not as sensitive in vivo to ASG-15ME, or other SLITRK6 specific ADCs, as the CHP-212 cell line. Because of this CHP-212 was chosen as the standard cell line for in vitro cytotoxicity assays. The data generated showed a dose-dependent inhibition of CHP-212 cell survival after treatment with ASG-15ME. The IC_{50} for ASG-15ME was calculated to be 0.99 nM. ASG-15ME had no effect on IGR-OV1 cells (SLITRK6 negative) when applied at the same concentrations. The MMAE conjugated isotype control antibody did not show any inhibitory activity in either of the cell lines tested.

Immunohistochemical Analysis of SLITRK6 Expression in Xenograft Models

Several xenografts were positive for SLITRK6 and two CDXs (SW-780 and RT-4) along with two PDXs (AG-B7 and AG-B8) were selected for in vivo efficacy studies due to their strong and homogenous expression even after multiple passages. Data with RT-4, AGB7 and AGB8, making up the bladder cancer panel, are reported here. RT-4 had an H-score of 280 with 100% of the tumor showing moderate to strong expression of SLITRK6. AG-B7 had an H-score of 230 with 85% of tumor with moderate to strong SLITRK6 expression and AG-B8 had an H-score of 250 with 90% of tumor having moderate to strong expression of SLITRK6. Because lung cancer is a potential indication for ASG-15ME treatment, we also identified a lung CDX model (NCI-322M) which was positive for SLITRK6. Expression was strong but not homogenous. This xenograft had an H-score of 185 with only 60% of the tumor cells having moderate to strong SLITRK6 expression and 5% of the tumor cells were negative. Expression of SLITRK6 in all xenografts is shown in inset picture alongside growth curves shown in Figure 4.

SLITRK6 Specific ADCs, Including ASG-15ME, Cause Potent Inhibition of Multiple Xenografts

In early studies in bladder CDX models we were able to show superior in vivo activity of AGS-15C conjugated with MMAE or MMAF when compared to the other antibodies in the lead panel. Figure 4a shows the activity of ASG-15ME and AGS-15MF compared with 3 of the antibodies in the lead panel. After a single 5mg/kg dose, both the MMAE and MMAF variants were able to cause significant tumor growth regressions of 49% ($p = 0.0015$) and 10% ($p = 0.3265$) for ASG-15ME and AGS-15MF respectively. The next most efficacious ADC was Ha15-10ac14E which caused a tumor regression of 16% ($p=0.0992$). The MMAF variant caused significant inhibition ($p=0.0002$) but did not cause regression. Due to this we selected AGS-15C as the lead antibody and carried out additional experiments designed to enable the selection of MMAE or MMAF as the payload for AGS-15C.

In the bladder PDX model AG-B7, ASG-15ME was significantly more efficacious than AGS-15MF ($p<0.0087$) when dosed bi-weekly at 5 mg/kg (Figure 4b). Statistics were calculated at day 21 at which point ASG-15ME demonstrated significant tumor regression of 45% ($p < 0.0001$). Neither of the isotype control ADCs caused tumor growth inhibition when compared to the vehicle control.

Dose ranging studies were carried out using the AG-B8 PDX model in which ASG-15ME and AGS-15MF were dosed at 0.5 and 0.25 mg/kg two times per week. In this study 0.25mg/kg was an effective dose for both ADCs but only ASG-15ME dosed at 0.5 mg/kg was able to cause regression (23% on day 16, $p = 0.0025$) and no regression with AGS-15MF at this dose (Figure 4c).

Because SLITRK6 is also expressed in a sub-set of lung cancer specimens, studies were carried out in the lung cancer xenograft model, NCI-H322M. In this study, ASG-15ME was significantly better than ASG-15MF at inhibiting tumor growth ($p < 0.0001$) and was able to cause 99% tumor growth inhibition. In contrast, AGS-15MF caused 43% tumor growth inhibition but this was not statistically significant ($p=0.0516$) compared to the control. The final measurement was taken on day 20 and dosing was 3mg/kg, two times per week, for a total of 5 doses (Figure 4d).

Discussion

With two approved ADCs and over 40 others in clinical development (22) significant advances have been made in recent years to bring ADC technology to the forefront of drug development. These advances have been made possible through improved drug conjugation technologies and better tumor targeting. In light of these improvements we have developed ASG-15ME, a potent MMAE-based ADC specific for SLITRK6. We have shown SLITRK6 to be highly expressed in non-invasive and invasive bladder cancer as well as in a sub-set of lung cancer, breast cancer and glioblastoma specimens. ASG-15ME was chosen after extensive in vitro characterization and in vivo evaluation in multiple xenograft models including four bladder and one lung xenograft model. ASG-15ME showed excellent anti-tumor activity in vivo with significantly better activity than other SLITRK6-specific ADCs tested. Although we observed activity with AGS-15MF, when compared head-to-head with ASG-15ME in bladder tumor models, ASG-15ME showed consistently higher activity often causing tumor regression when AGS-15MF caused only tumor growth inhibition. The activity of AGS-15MF was still significant so we continued to compare the activity of MMAE versus MMAF as there was evidence that the choice of a non-cleavable linker may be better than a cleavable linker in some tumor types (23).

We extended our studies into xenograft models where SLITRK6 is not homogenously expressed. In one such model, NCI-H322M (lung cancer xenograft), ASG-15ME caused complete tumor growth inhibition whereas AGS-15MF did not cause significant growth inhibition. In this model there is heterogeneous expression of SLITRK6 with approximately 5% of tumor cells being completely negative. The results we observed suggest that even the negative tumor cells and those expressing low levels of SLITRK6 were killed by treatment with ASG-15ME. We thought this an important observation because not all patient tumors will have the same homogeneity at the genetic and histological level as seen in our bladder cancer xenografts (24). The high potency of ASG-15ME in regressing tumors with homogenous as well as heterogeneous expression, taken together with other data, led to the selection of MMAE as the payload for our drug product. Furthermore, at the time when the selection was made, more was known about the activity and safety of MMAE in the clinic compared to MMAF. This choice may be important if we extend our clinical studies into other tumor types where we see SLITRK6 expression, such as lung cancer, breast cancer and glioblastoma. The activity seen in non-homogenous tumors is most likely due to the ability of some ADCs with cleavable linkers to cause bystander cell killing (25). This is where cells that do not express the target, or express low levels of the target, are killed by MMAE, that once cleaved, is able to diffuse across cell membranes and enter other cells in the tumor milieu (26). This type of bystander killing is not as likely with MMAF based conjugates as MMAF was designed to have an additional carboxyl group giving it a negative charge at neutral pH. Furthermore, MMAF is linked via a non-cleavable linker so the released active metabolite is cysteine-linker-MMAF (cys-MMAF) thus retaining the charged amino and carboxyl groups of the amino acid (25). These charged carboxyl and amino groups make MMAF metabolites less able to diffuse across the cell membrane (19). We speculate that this difference

in membrane permeability is the likely reason for the difference seen in activity with ASG-15ME versus AGS-15MF in xenograft models with non-homogenous SLITRK6 expression. Additional experiments would need to be carried out to prove this.

This is the first report that SLITRK6 is highly expressed in advanced transitional cell bladder cancer and other cancers of epithelial origin as well as on transitional epithelium of normal bladder and ureter. Gene analysis in mouse embryos suggest that SLITRK6 may be expressed in multiple organs but there are no data to indicate that it is expressed in the urinary tract (14) and SLITRK6 knock-out mice are not reported to have any urinary tract defects (16). Although the level of SLITRK6 see in normal transitional epithelium is often as high as that seen in bladder cancer, the risk of bladder related on target toxicity may be mitigated by the fact that patients with advanced bladder cancer may have undergone radical cystectomy as a first line of therapy (27, 28).

We also saw staining in other normal tissues such as adrenal gland, stomach, pancreas, breast and lung. While RNA studies suggest that SLITRK6 may be expressed in these organs in embryonic development (13, 29) and even in adult lung (14), the staining that we saw in these organs was cytoplasmic, weak and often appeared to be non-specific. With this in mind we believe that SLITRK6 has a favorable tumor to normal expression profile making it a suitable target for ADC therapy but despite this, selection of a cyno-cross-reactive mAb was very important to confirm that such normal expression was in fact tolerated.

Bladder cancer is one of the tumors associated with the highest morbidity and mortality. It is the second most common urological cancer and is characterized by high recurrence rates and poor prognosis (30). Treatment options for patients with advanced bladder cancer are limited and the five year survival rate decrease dramatically as the disease progresses. Although survival rates

are increasing with early diagnosis and the introduction of neoadjuvant therapy prior to surgery (12, 31) new treatments are still needed as recurrence rates are high even after intensive therapy. In summary, we have shown that SLITRK6 is highly expressed in bladder cancer and other tumors of epithelial origin. We have developed ASG-15ME, a human monoclonal antibody conjugated to MMAE through a cleavable linker, to target SLITRK6. ASG-15ME induced potent inhibition, and even tumor regression, in multiple xenografts. These findings show that SLITRK6 is a novel target in bladder cancer and preclinical data support the evaluation of ASG-15ME (Product name AGS15E) in Phase I clinical trials, which are currently underway in advanced urothelial cancer.

Acknowledgements

Agensys Inc, is a wholly owned affiliate of Astellas.

ASG-15ME is being co-developed in conjunction with Agensys' partner, Seattle Genetics (Headquarters; 21717 - 30th Drive S.E., Building 3, Bothell, WA 98021).

References

1. Younes A, Bartlett NL, Leonard JP, Kennedy DA, Lynch CM, Sievers EL et al. Brentuximab vedotin (SGN-35) for relapsed CD30-positive lymphomas. N. Engl. J. Med 2010; 363: 1812–1821.
2. Senter, P. and Sievers, E.L. The discovery and development of brentuximab vedotin for use in relapsed Hodgkin lymphoma and systemic anaplastic large cell lymphoma. Nat. Biotechnol 2012; 30: 631–637.
3. Lopus M, Oroudjev E, Wilson L, Wilhelm S, Widdison W, Chari R et al. Maytansine and cellular metabolites of antibody-maytansinoid conjugates strongly suppress microtubule dynamics by binding to mictotubules. Mol. Cancer Ther 2010; 9(10); 2689-2699.
4. LoRusso PM, Weiss D, Guardino E, Girish S, Sliwkowski MX. Trastuzumab emtansine: a unique antibody–drug conjugate in development for human epidermal growth factor receptor 2-positive cancer. Clin. Cancer Res 2011; 17: 6437–6447.

5. Verma S, Miles D, Gianni L, Krop IE, Welslau M, Baselga J et al. Trastuzumab emtansine for HER2-positive advanced breast cancer. N. Engl. J. Med 2012; 367: 1783-1791.
6. English DP, Roque DM and Santin AD. Her-2 expression beyond breast cancer: therapeutic implications for gynecological malignancies. Mol Diagn Ther. 2013; 17(2): 85-99.
7. Vaklavas C. and Ferero-Torres A. Safety and efficacy of brentuximab vedotin in patients with Hodgkin lymphoma or systemic anaplastic large cell lymphoma. Ther Adv Hem. 2012; 3(4): 209-225.
8. Ferlay J, Soerjomataram I, Dikshit R, Eser S, Mathers C, Rebelo M et.al. Cancer incidence and mortality worldwide: sources, methods and major patterns in GLOBOCAN 2012. Int J Cancer. 2015: 1;136(5):E359-86.
9. American Cancer Society. Cancer Facts and Figures 2013. Atlanta GA: American Cancer Society; 2013
10. Soloway M.S. It is time to abandon the "superficial" in bladder cancer. Eur Urol. 2007; 52(6): 1564–5
11. Edge SB, Byrd DR, Compton CC, Fritz A, Greene F and Trotti A, eds.: AJCC Cancer Staging Manual. 7th ed. New York, NY: Springer, 2010, pp 497-505.
12. Sherif A, Holmberg L, Rintala E, Mestad O, Nilsson J, Nilsson S et al. Neoadjuvant cisplatinum based combination chemotherapy in patients with invasive bladder cancer: a combined analysis of two Nordic studies. Eur Urol 2004: 45(3): 297-303.
13. Aruga J, Mikoshiba K. Identification and characterization of Slitrk, a novel neuronal transmembrane protein family controlling neurite outgrowth. Mol Cell Neurosci. 2003; 24: 117-129.
14. Aruga J, Yokota N, Mikoshiba K. Human SLITRK family genes: genomic organization and expression profiling in normal brain and brain tumor tissue. Gene 2003; 317: 87-94.
15. Katayama K, Zine A, Ota M, Matsumoto Y, Inoue T, Fritzsch B et al. Disorganized innervations and neuronal loss in inner ear of Slitrk6-deficient mice. PLoS One 2009; 4(11): e7786.
16. Matsumoto Y, Katayama K, Okamoto T, Yamada K, Takashima N, Nagao S et al. Impaired auditory-vestibular functions and abnormalities of Slitrk6-deficient mice. PLoS One 2011; 6(1):e16497.
17. Tekin M, Chioza BA, Matsumoto Y, Diaz-Horta O, Cross HE, Duman D et al. SLITRK6 mutations cause deafness in humans and mice. J. Clin. Invest 2013; 123(5): 2094-2102.
18. McCarty K, Szabo E, Flowers J, Cox EB, Leight GS, Miller L et al. Use of monoclonal anti-estrogen receptor antibody in the immunohistochemical evaluation of human tumors. Cancer Research 1986; 46: 4424s-4428s.
19. Doronina SO, Toki BE, Torgov MY, Mendelsohn BA, Cerveny CG, Chance DF, et.al. Development of potent monoclonal antibody auristatin conjugates for cancer therapy. Nat Biotechnol 2003; 21:778-84.

20. Doronina SO, Mendelsohn BA, Bovee TD, Cerveny CG, Alley SC, Meyer DL et al. Enhanced activity of monomethylauristatin F through monoclonal antibody delivery: effects of linker technology on efficacy and toxicity. Bioconjug Chem 2006;**17**:114–24.
21. Conover WJ, Iman RL. Rank transformations as a bridge between parametric and non-parametric statistics. The American Statistician 1981; 35(3): 124-129.
22. Mullard, A. Maturing antibody–drug conjugate pipeline hits 30. Nat. Rev. Drug Discov 2013; 12: 329–332.
23. Polson AG, Calemine-Fenaux J, Chan P et al. Antibody-Drug Conjugates for the Treatment of Non–Hodgkin's Lymphoma: Target and Linker-Drug Selection. Cancer Res. 2009; 69:2538.
24. Bedard PL, Hansen AR, Ratain MJ, Siu LL. Tumor heterogeneity in the clinic. Nature 2013; 501: 355-364.
25. Kovtun YV, Goldmacher VS. Cell killing by antibody drug conjugates. Cancer Lett. 2007; 255: 232-240.
26. Okeley NM, Miyamoto JB, Zhang x, Sanderson RJ, Benjamin DR, Sievers EL et al. Intracellular activation of SGN-35, a potent anti-CD30 antibody-drug conjugate. Clin Cancer Res 2010; 16: 888-897.
27. Richie JP: Surgery for invasive bladder cancer. Hematol Oncol Clin North Am 1992: 6 (1) 129-45.
28. Lerner SP, Schoenberg MP, Sternberg CN. Treatment and management of bladder cancer 2008; Informa Healthcare Press: ISBN 10: 0 415 46217 7.
29. Aruga j. Slitrk6 expression in mouse embryo and its relationship to that of Nlrr3. Gene expression patters 2003; 3: 727-733.
30. Kausch I, Böhle A. Bladder cancer II Molecular aspects and diagnosis. Eur Urol. 2001; 5: 498–506.
31. Winquist E, Kirchner TS, Segal R, Chin J, Lukka H. Neoadjuvant chemotherapy for transitional cell carcinoma of the bladder: a systematic review and meta-analysis. J Urol 2004: 171 (2): 561-9.

Table 1. SLITRK6 expression in bladder cancer and normal tissue

Table 1a. SLITRK6 Expression in Bladder Cancers According to Histopathological Diagnosis

Cancer	Percentage Ratio of Cancers in Each Final Score Category				Overall Positive Ratio	Total Cases
	Strong	Moderate	Low	Negative		
Bladder transitional cell carcinoma	37%	35%	18%	10%	90%	452
Bladder metastatic cancers	71%	24%	5%	0%	100%	18
Bladder other types of cancers	3%	10%	41%	46%	54%	39

Table 1b. SLITRK6 Expression in Bladder Cancers According to TNM (tissue-node-metastasis) Grading

	H-score 200-300	H-score 100-199	H-score 15-99	H-score 0-14
TNM 0-1	44	53	21	7
	35%	42%	17%	6%
TNM 2-4	87	108	75	30
	29%	36%	25%	10%

Table 2. Summary of SLITRK6 Expression in Normal Human Tissues

Organ, Tissue/Cell	No. of Positive / Total Cases
Adrenal gland	6/6
Bladder, transitional epithelium	3/3
Breast, alveoli and ducts	1/6
Bone marrow	0/1
Brain	0/15
Colon, glands	3/6
Esophagus, squamous epithelium	0/6
Eye	0/4
Fallopian tube	0/3
Heart	0/6
Kidney, subset of renal tubules	0/9
Larynx, squamous epithelium	1/3
Liver, bile ducts	0/6
Lung, bronchiolar epithelium	3/6
Mesothelium	0/3
Nerve	0/3
Ovary	0/6
Pancreas, ducts	5/6
Parathyroid	0/4
Pituitary gland, endocrine cells	0/4
Placenta, trophoblasts	3/3
Prostate, some glands	0/6
Rectum, glands	1/3
Salivary gland, ducts	0/3
Skeletal muscle	0/6
Skin, epidermis, sweat glands, hair follicles	0/5
Small intestine, glands	0/5
Spinal cord	0/2
Spleen	0/5
Stomach, glands	6/6
Testis, Leydig cells and seminiferous tubules-lining cells	0/6
Thymus, corpuscle cells	0/6
Thyroid	4/6
Tonsil, squamous epithelium	0/6
Ureter, transitional epithelium	2/2
Uterus, cervix, squamous epithelium	0/5
Uterus, endometrium, glands	0/5

Table 3. Comparison of the 7 lead monoclonal antibodies from which AGS-15C was selected. Selection was made from a panel of gamma 1 and gamma 2 antibodies with sub-nanomolar binding affinities representing different epitope bins. Epitope bins were determined by competition binding studies. All antibodies cross-react with cynomolgus macaque (cyno) SLITRK6 with high affinity.

mAb Name	Isotype	Epitope	Affinity, human (nM)	Affinity, cyno (nM)
AGS15C	γ2	37	0.005	0.01
Ha15-10ac14	γ2	36	0.142	0.08
Ha15-1abe48	γ1	13	0.02	0.013
Ha15-1abe16	γ1	11	0.03	0.011
Ha15-6bd30	γ1	31	0.009	0.025
Ha15-1abe40	γ1	7	0.08	0.021
Ha15-1c25	γ1	8	0.004	0.02

Table 4. Affinity constants for AGS-15C compared with 3 lots of ASG-15ME shows no loss in binding after conjugation with MMAE

ADC	LOT	Bmax (MFI)	Kd (nM)
AGS-15C	1396-63A	179	0.015
ASG-15ME	1389-39-A	202	0.018
ASG-15ME	15c-vcE-01	187	0.012
ASG-15ME	1264-100	181	0.011

Values in Table 4 were calculated as follows; MFI values were entered into Graphpad Prisim software and analyzed using the one site binding (hyperbola) equation of Y=Bmax*X/(Kd+X) to generate saturation curves. Bmax is the MFI value at maximal binding of each antibody to SLITRK6 and Kd is the concentration of each antibody required to reach half-maximal binding.

Figure Legends;

Figure 1. SLITRK6 expression in transitional cell carcinoma of the bladder at various stages

(A) SLITRK6 expression on the membrane of tumor cells. Positive membrane can be seen as a dark brown ring around a blue counterstained nucleus. Some cytoplasm staining in the tumor cells can also be seen. Inset shows strong membrane staining pattern.

(B) SLITRK6 expression in transitional cell bladder cancer in situ (T_1).

(C) SLITRK6 expression in invasive bladder cancer that has invaded the muscle layer of the bladder (T_2).

(D) SLITRK6 expression in invasive bladder cancer that has invaded the muscle layer grown through the bladder muscle into the fat layer surrounding the bladder (T_3).

(E) SLITRK6 expression in metastatic bladder cancer. In all cases, SLITRK6 expression is strong, epithelial and homogenous.

Figure 2. SLITRK6 expression in normal tissues

(A) SLITRK6 expression in the transitional epithelium of normal bladder. Inset picture at higher magnification shows that SLITRK6 expression is mostly membrane associated. A similar expression pattern was seen in transitional epithelium of ureter.

(B) SLITRK6 expression in adrenal glad was cytoplasmic and weak in most cases. Inset picture at higher magnification shows staining to be diffuse and cytoplasmic. In contrast to transitional epithelium of the bladder and ureter, no membrane staining was seen.

(C) SLITRK6 expression in stomach. Staining was mostly cytoplasmic, with weak to moderate intensity in glandular epithelium of the basal mucosa.

(D) SLITRK6 expression in pancreas. Inset picture at higher magnification shows positive acinar cells but staining is cytoplasmic. No membrane staining was seen.

(E) SLITRK6 expression in lung, colon and breast. Staining was weak, cytoplasmic and sparse and appeared to be non-specific.

(F) Examples of organs where interstitial, mast cell like, cells were positive for SLITRK6. Multiple, isolated, cells can be seen in each section and 2 examples are high-lighted with red arrows.

Figure 3. Internalization of ASG-15ME examined by confocal microscopy

Figure 3a.

The left panel shows incubation at 4^0C with distinct cell surface localization with minimal evidence of internalization (green). The right panel shows incubation after 1 hour at 37^0C with membrane localization of ASG-15ME dramatically reduced and distribution of the ADC in discrete punctate intracellular aggregates throughout the cytosol (green). The nucleus can be seen stained with TOPRO®-3 Iodide (blue/green).

Figure 3b.

Cytosolic/internalized ASG-15ME can be seen co-localized with EEA1 (top panel) and LAMP1 (bottom panel) after 30minutes at 37^oC. Co-localization can be seen when the red signal from ASG-15ME merges with the green signal from EAA1 or LAMP1 to give a yellow signal. These can be seen most clearly in the Z-stack overlays as depicted by the white arrows.

Figure 3c.

FACS histogram showing representative binding of ASG-15ME (Lot # 1389-39A in Table 3) to SW780 cells. The purple profile shows binding of ASG-15ME (B_{max} , 202, Kd 4.4nM) and the green profile shows the isotype control.

Figure 4. ASG-15ME showed potent antitumor activity in multiple xenograft models in vivo

(A) Efficacy of ASG-15ME and ASG-15MF compared to three other SLITRK6 specific ADCs in an RT-4 CTX study. ASG-15ME showed superior activity after a single 5mg/kg dose administered intravenously (i.v.) when tumors had reached a volume of approximately 230mm^3. The study was terminated at day 31 when the tumors in the control groups exceeded 1000mm^3 (n+5 for each cohort).

(B) In multiple dose studies in the AG-B7 PDX, ASG-15ME was able to cause a 45% tumor regression ($p < 0.0001$) when dosed i.v. at 0.5mg/kg, 2 x per week. The last dose was given on day 21 and the study was terminated when the control group tumor volume was over 1000mm^3.

(C) ASG-15ME was highly efficacious when dosed at 0.25mg/kg, 2 x per week i.v in AG-B8 PDX. Dosing started when tumors reached a volume of approximately 200mm^3 (N=7). The last dose was given on day 14.

(D) In the lung xenograft model, NCI-H322M, ASG-15ME was significantly more efficacious than ASG-15MF and was able to cause 99% tumor growth inhibition ($p <0.0001$) . Although ASG-15MF was able to cause 43% tumor growth inhibition this

was not statistically significant (p=0.0516). Dosing started when tumors reached a volume of approximately 200mm^3 and were given 2x per week at 3mg/kg (n=6). The final dose was given on day 17. Note the IHC inset showing SLITRK6 expression in NCI-H322M. Expression is heterogeneous and negative tumor cells can be seen within section.

Figure 1

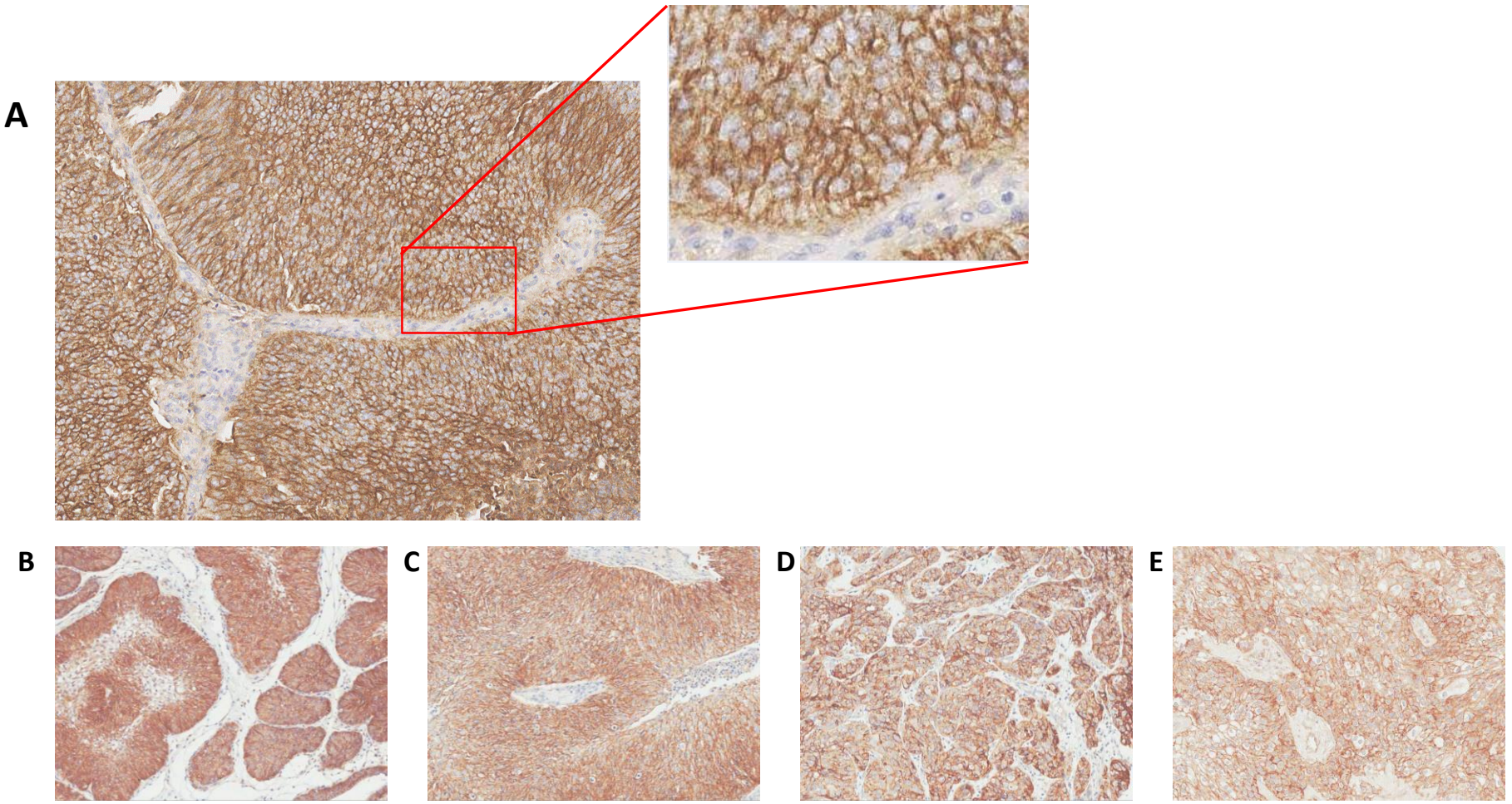

Figure 2

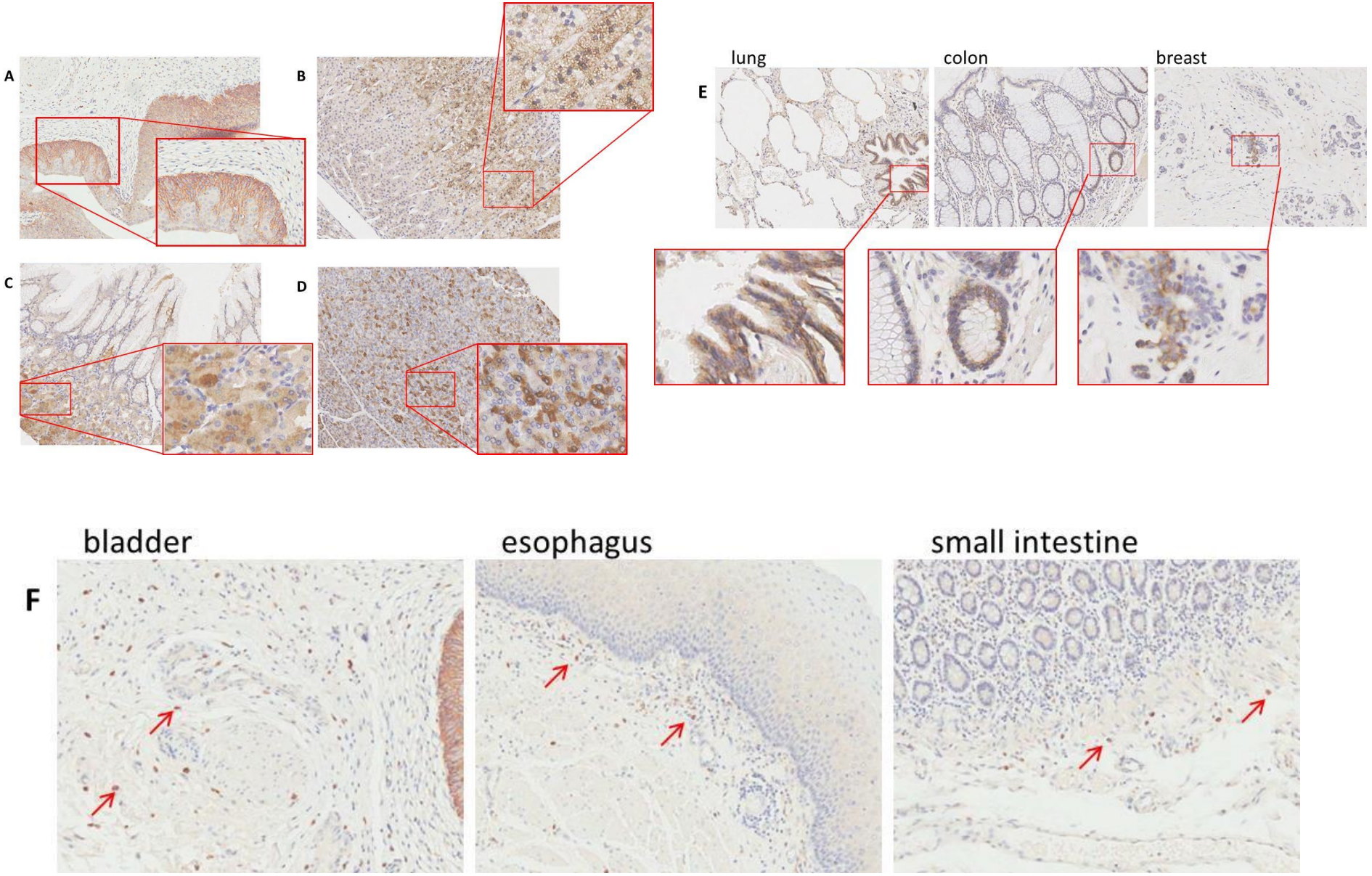

Figure 3

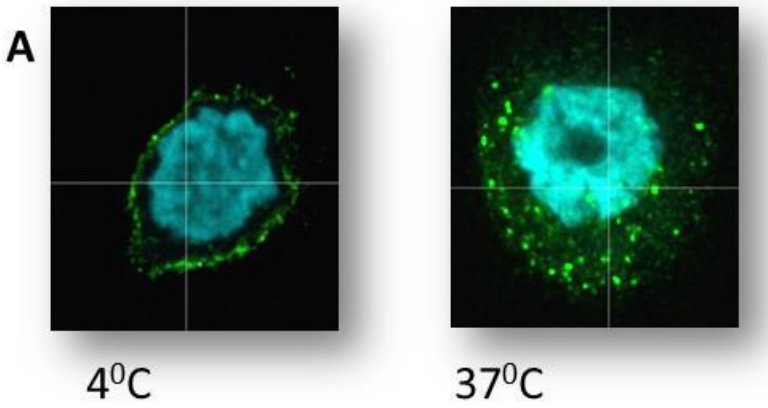

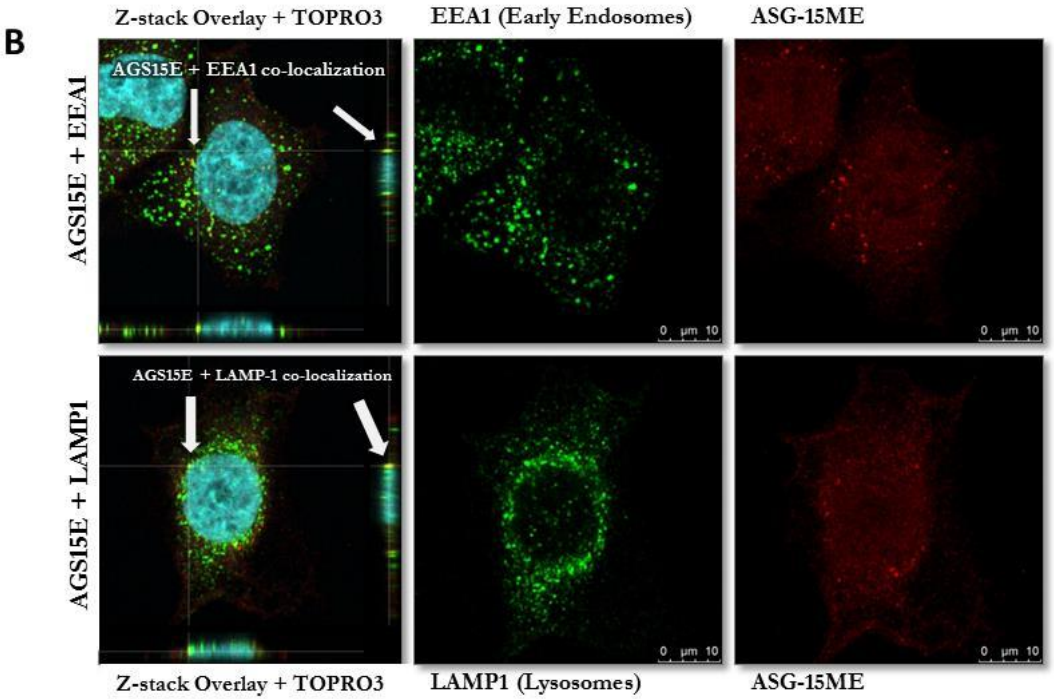

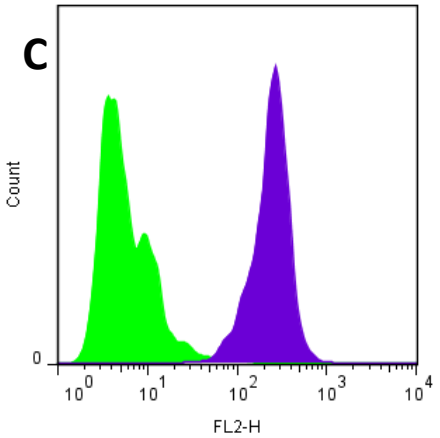

Figure 4

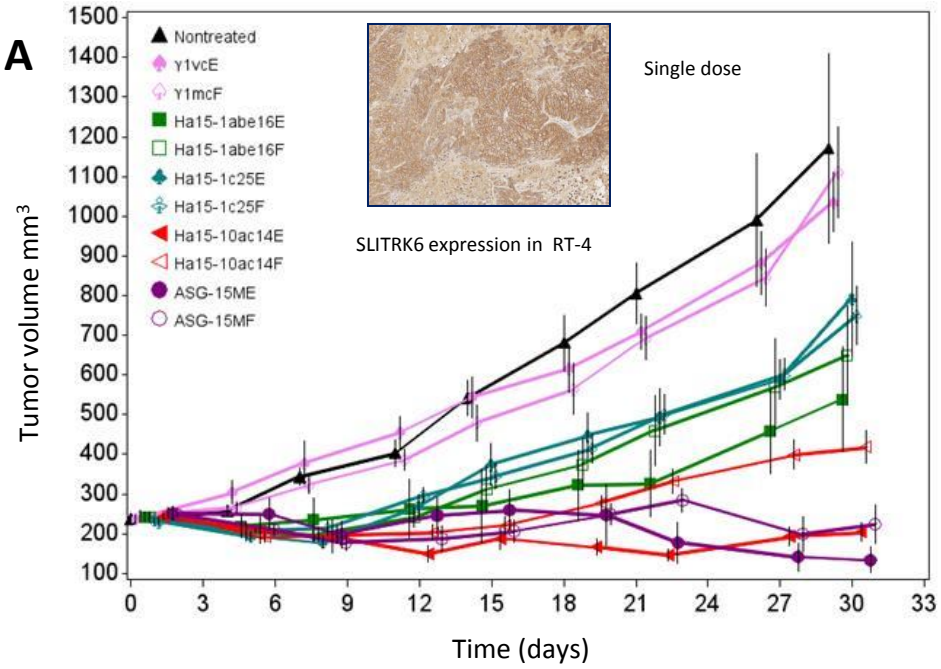

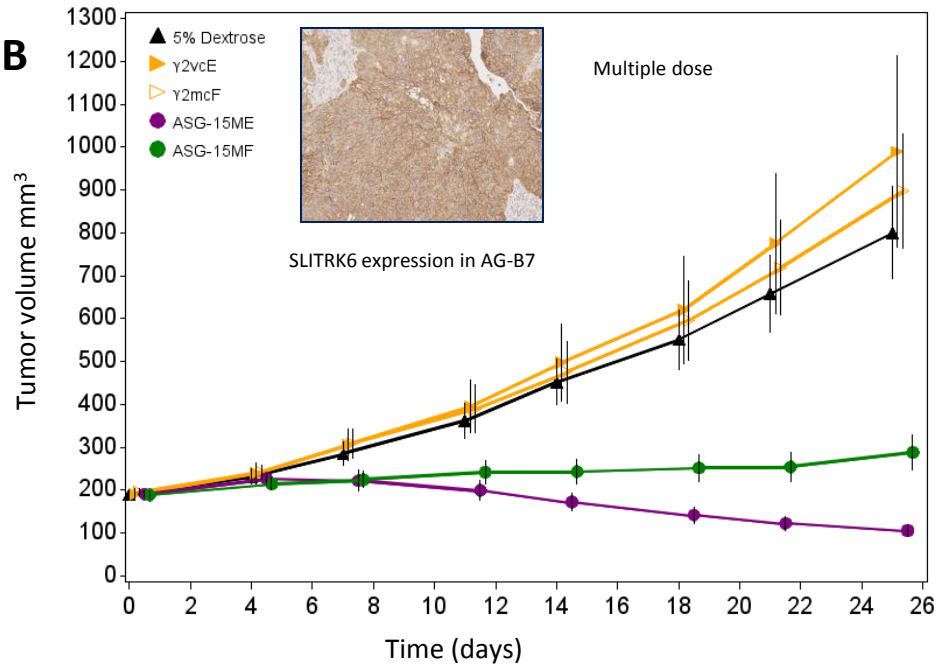

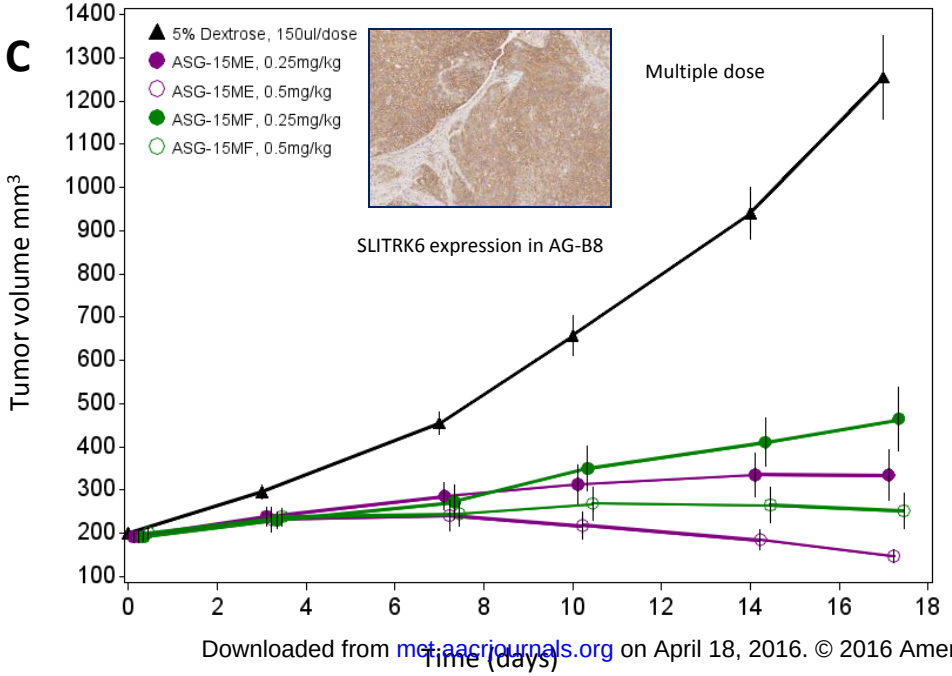

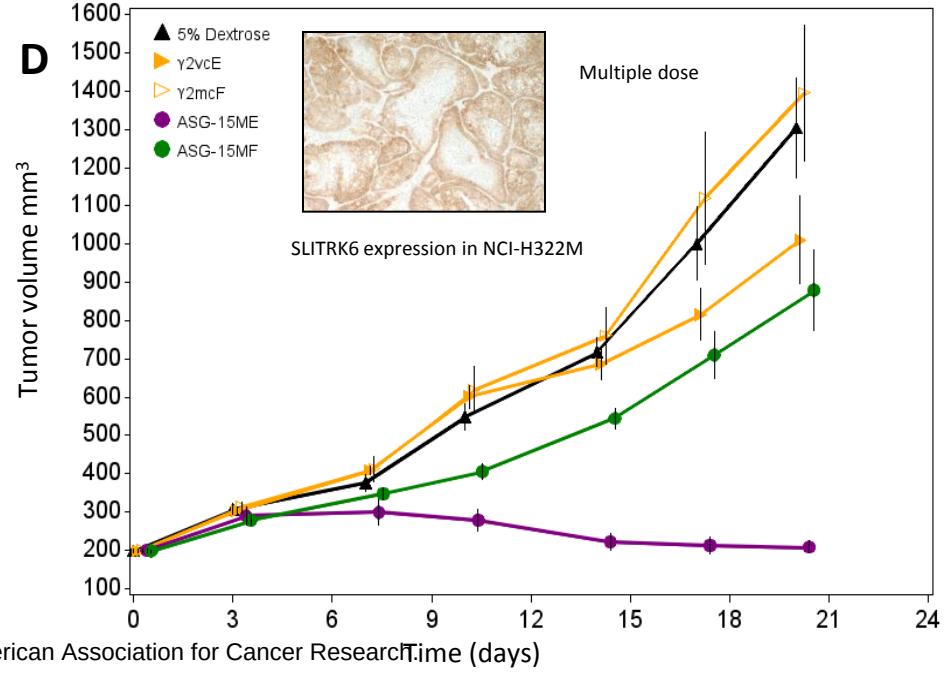

AACR American Association for Cancer Research

Molecular Cancer Therapeutics

Development of ASG-15ME, a Novel Antibody Drug Conjugate Targeting SLITRK6, a New Urothelial Cancer Biomarker

Kendall Morrison, Pia M. Challita-Eid, Arthur Raitano, et al.

Mol Cancer Ther Published OnlineFirst March 4, 2016.